Cell Host & Microbe
Article

Host Scavenger Receptor SR-BI Plays a Dual Role in the Establishment of Malaria Parasite Liver Infection

Cristina D. Rodrigues,[1,2,8] Michael Hannus,[3,8] Miguel Prudêncio,[1,2,8] Cécilie Martin,[3] Lígia A. Gonçalves,[2] Sílvia Portugal,[1] Sabrina Epiphanio,[1] Akin Akinc,[4] Philipp Hadwiger,[5] Kerstin Jahn-Hofmann,[5] Ingo Röhl,[5] Geert-Jan van Gemert,[6] Jean-François Franetich,[7] Adrian J.F. Luty,[6] Robert Sauerwein,[6] Dominique Mazier,[7] Victor Koteliansky,[4] Hans-Peter Vornlocher,[5] Christophe J. Echeverri,[3] and Maria M. Mota[1,2,*]
[1]Unidade de Malária, Instituto de Medicina Molecular, Universidade de Lisboa, 1649-028 Lisboa, Portugal
[2]Instituto Gulbenkian de Ciência, 2780-156 Oeiras, Portugal
[3]Cenix BioScience GmbH, Tatzberg 47, 01307 Dresden, Germany
[4]Alnylam Pharmaceuticals, 300 Third Street, Cambridge, MA 02142, USA
[5]Roche Kulmbach GmbH, Fritz-Hornschuch-Strasse 9, 95326 Kulmbach, Germany
[6]Department of Medical Microbiology, University Medical Centre, P.O. Box 9101, 6500 HB Nijmegen, The Netherlands
[7]Inserm U511, Université Pierre et Marie Curie-Paris, Centre Hospitalier Universitaire Pitié-Salpêtrière, F-75013 Paris, France
[8]These authors contributed equally to this work
*Correspondence: mmota@fm.ul.pt
DOI 10.1016/j.chom.2008.07.012

SUMMARY

An obligatory step of malaria parasite infection is *Plasmodium* sporozoite invasion of host hepatocytes, and host lipoprotein clearance pathways have been linked to *Plasmodium* liver infection. By using RNA interference to screen lipoprotein-related host factors, we show here that the class B, type I scavenger receptor (SR-BI) is the strongest regulator of *Plasmodium* infection among these factors. Inhibition of SR-BI function reduced *P. berghei* infection in Huh7 cells, and overexpression of SR-BI led to increased infection. In vivo silencing of liver SR-BI expression in mice and inhibition of SR-BI activity in human primary hepatocytes reduced infection by *P. berghei* and by *P. falciparum*, respectively. Heterozygous *SR-BI*$^{+/-}$ mice displayed reduced *P. berghei* infection rates correlating with liver SR-BI expression levels. Additional analyses revealed that SR-BI plays a dual role in *Plasmodium* infection, affecting both sporozoite invasion and intracellular parasite development, and may therefore constitute a good target for malaria prophylaxis.

INTRODUCTION

Malaria is a major global health problem, found most acutely in Sub-Saharan Africa and in some parts of Asia and South America. Each year there are about 600 million new clinical cases and at least one million individuals, mostly children, die from malaria infections (Greenwood and Mutabingwa, 2002), all of which are caused by the protozoan parasite *Plasmodium*. Moreover, malaria represents a serious burden on the economic potential of many countries in the world. Various attempts at eradicating this disease have so far been unsuccessful, and in fact within the last 10 to 15 years the burden of malaria has been increasing (Greenwood and Mutabingwa, 2002), mainly because of the emergence of *P. falciparum* variants that are resistant to the drugs in use (Cunha-Rodrigues et al., 2006). These realities have compounded the urgency of finding novel treatment strategies that will be less vulnerable to the development of parasite resistance, a goal that necessarily requires a better understanding of the underlying parasite-host interactions.

After the bite of an infected mosquito delivers *Plasmodium* sporozoites into a human host, the parasite first accumulates in the liver, where it migrates through the cytoplasm of several hepatocytes before invading the one in which it will develop into an exoerythrocytic form (EEF) (Mota et al., 2001). During this asymptomatic liver infection, the parasite proliferates and changes from a motile sporozoite into thousands of merozoites that will be released in the bloodstream and infect red blood cells, initiating the clinical phase of infection. In doing so, its exploitation of host liver resources represents an important and as-yet underinvestigated vulnerability to prophylactic intervention. In fact, although a single surviving EEF is sufficient to give rise to a blood stage malaria infection, it has been shown that even a small reduction in the liver parasite load can lead to an even greater decrease in malaria severity (Alonso et al., 2005).

In this context, it is our main interest to identify and characterize the role of host factors that influence *Plasmodium* liver infection, as these may contribute to the design of rational interventional strategies for the development of novel prophylactic agents. To this end, we have established a high-throughput assay system that, combined with high-content readouts using automated microscopy, we have used for RNA interference (RNAi) screening experiments. The present study was initiated to follow up on observations from earlier reports that suggested a link between host lipoprotein clearance pathways and *Plasmodium* sporozoite infection of the liver (Shakibaei and Frevert, 1996; Sinnis et al., 1996). These reports have suggested a link between hepatocyte invasion by sporozoites and apolipoprotein clearance in the liver. However, from these reports, it was not

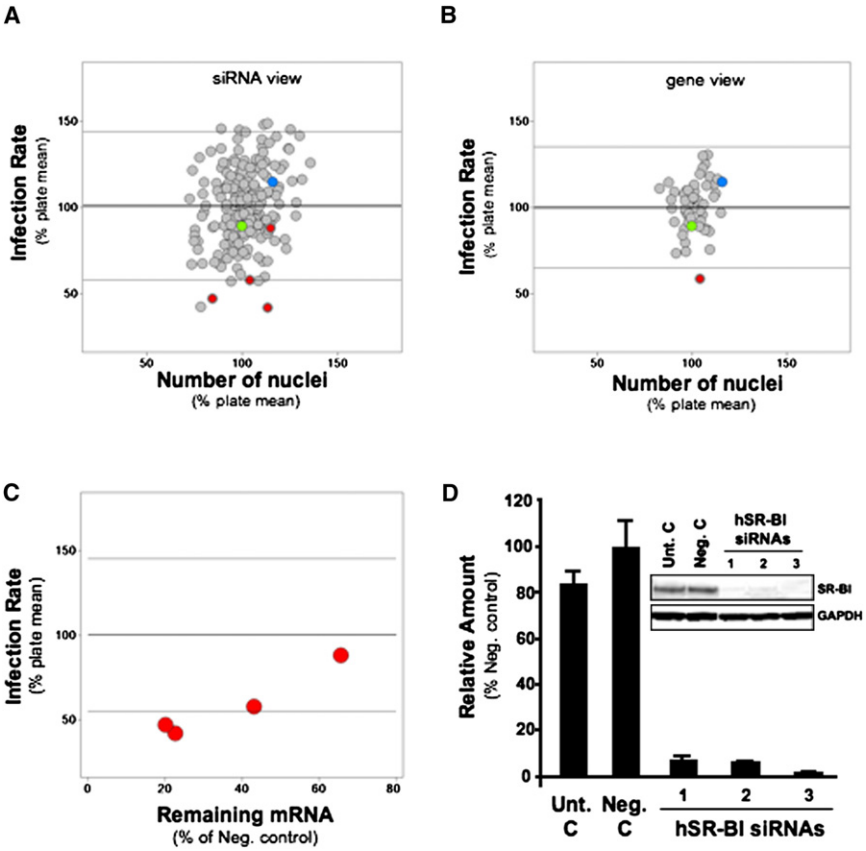

Figure 1. RNAi Screen of Lipoprotein Pathway Genes Identifies Host SR-BI as Required for Infection of Huh7 Cells by *P. berghei* Sporozoites

(A) Effects of 206 siRNA treatments targeting 53 lipoprotein pathway genes on Huh7 cell proliferation (x axis) and infection by *P. berghei* sporozoites (y axis), both measured 24 hr after sporozoite addition and 72 hr after siRNA transfection. Cell proliferation was estimated as the percentage of Huh7 nuclei relative to the mean from all experimental wells on each plate. Infection rates were calculated for each sample, as well as number of EEFs:cell confluency (as described in main text), also plotted here as a percentage relative to the mean from all experimental wells on each plate. For convenience, horizontal lines marking ± 2 SD of the whole data set are also shown. Each circle represents one siRNA (mean of triplicate values, see also Table S1 for exact values). Negative controls appear as blue and green circles, corresponding to untreated cells and cells transfected with a nonspecific control siRNA, respectively. Red circles correspond to siRNAs targeting *SR-BI*.

(B) Same dataset as shown in (A), with each circle representing one of the 53 tested genes, and corresponding to the mean value from all siRNAs targeting each gene. Color attributions are the same as in (A).

(C) Comparison of effects of *SR-BI* siRNA treatments on infection rate versus remaining mRNA levels. Each circle represents one *SR-BI* siRNA (mean of triplicate values). The horizontal gray lines represent 2 SD from the mean infection rate for entire data set.

(D) Effect of siRNA treatments on SR-BI protein levels in Huh7 cells, measured by semiquantitative western blotting of extracts taken at the time of infection, i.e., 48 hr after siRNA transfection, from untransfected cells (Unt. C), cells transfected with a negative control nonspecific siRNA (Neg. C), or cells transfected with human *SR-BI*-specific siRNAs (*hSR-BI* siRNAs). GAPDH was used as a loading control. Results were normalized to Neg. C levels (100%) and are expressed as the mean ± SD of SR-BI expression levels in three independent samples.

clear whether a lipoprotein receptor was involved in the infection process or not. Thus, we sought to determine whether this was the case, following an unbiased RNAi-based approach.

RESULTS

Host Scavenger Receptor BI Is Required for *P. berghei* Infection of Huh7 Cells

We sought to analyze the role of lipoprotein pathway genes in the liver stage of *Plasmodium* infection by applying an in vitro infection assay in the context of a systematic RNAi-induced loss-of-function screen. To this end, we assembled a library of 206 siRNAs targeting 53 genes expressed in the liver and annotated as having validated or putative roles in lipoprotein assembly, binding, or uptake (Table S1 available online). Each gene was targeted with at least three distinct siRNA sequences, and each siRNA was transfected individually into human Huh7 hepatoma cells 24 hr after seeding, and, 48 hr later, cells were either infected with freshly isolated *P. berghei* sporozoites or lysed for quantitative RT-PCR (qRT-PCR) analysis of target mRNA knockdown levels at the onset of infection (Figure S1). We then quantified infection rates by fluorescence microscopy, using automated image analysis to count the number of stained EEFs, and normalizing these values to cell confluency, as determined by actin staining, to compensate for potential differences in total cell surface available for infection in each well.

This library of siRNAs was screened in two independent runs, generating phenotypic loss-of-function data and qRT-PCR analysis of remaining target mRNA levels (see detailed data in Table S1). One gene, scavenger receptor BI (*SR-BI*), stood out from the rest by showing significant reductions in infection rates with three distinct siRNA sequences (Figure 1A, $p < 0.001$). This is readily illustrated by plotting of the mean results from all siRNAs for each targeted gene (Figure 1B). This effect on infection occurred without any detectable side effects on cell proliferation, as measured by nuclear counts (Figure 1A, Table S1). Importantly, the multiplicity of siRNA sequences underlying this result argues strongly that the observed phenotype is indeed a specific consequence of downregulating SR-BI expression and is not arising through off-target effects (see Echeverri et al., 2006). As further confirmation of specificity, the phenotypic severity (i.e., degree of inhibition of infection) was found to correlate well with SR-BI knockdown, as quantified at the mRNA level by qRT-PCR (Figure 1C), with four distinct SR-BI-targeting siRNA sequences in multiple independent experiments. The SR-BI knockdown was also confirmed at the protein level by quantitative western

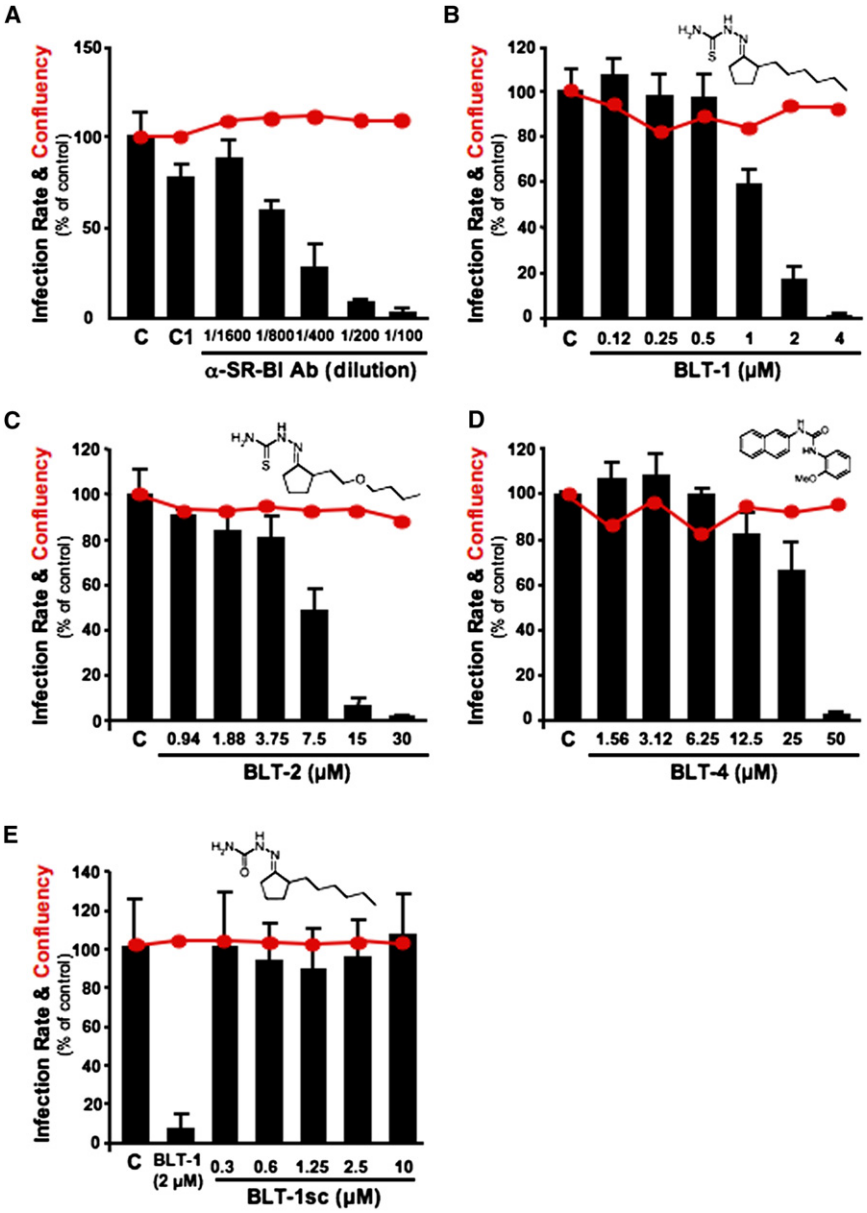

Figure 2. Inhibition of Host SR-BI Protein Function Reduces *P. berghei* Sporozoite Infection of Huh7 Cells

Antibody and all compounds were added to Huh7 cells 1 hr before sporozoite addition, and infection rates were measured 24 hr after sporozoite addition, by quantification of the number of EEFs, as described in the main text. Results are expressed as the mean ± SD of EEFs (%) in three independent infections. Red symbols and lines represent the mean levels of cell confluence based on automated analysis of actin staining, as measured for each set of triplicate samples.

(A) Effect of a serial dilution of a SR-BI-blocking antibody on *P. berghei* infection rate of Huh7 cells. "C1" indicates solvent-treated cells used as control. Cells treated with an irrelevant antibody (anti-tubulin) were used also as control ("C").

(B–D) Effect of known chemical inhibitors of SR-BI (BLT-1, BLT-2, and BLT-4, respectively) used at different concentrations on *P. berghei* infection rate in Huh7 cells, as measured by quantification of the number of EEFs. "C" indicates solvent-treated cells used as negative control. The chemical formula of each chemical inhibitor is also presented.

(E) Effect of different concentrations of the isostructural, but essentially inactive, semicarbazone derivative of BLT-1 (BLT-1sc) on *P. berghei* infection rate in Huh7 cells, as measured by quantification of the number of EEFs. "C" indicates solvent-treated cells used as negative control. The chemical formula of the compound is also presented.

blotting (Figure 1D). Together, these results strongly implicate SR-BI as a key host molecule playing an important role during *Plasmodium* infection of liver cells. It should be noted that the present data does not rule out the possible involvement of other genes among those tested here, as negative results in RNAi screens are generally inconclusive (see Echeverri et al., 2006).

The implication of SR-BI was further validated by testing the effects of known SR-BI inhibitors on infection, including a SR-BI-blocking antibody (Silver, 2002) and several small synthetic molecules previously reported to inhibit the SR-BI-mediated selective uptake of lipids from HDL (termed "blockers of lipid transport," or BLTs [Nieland et al., 2002]). Addition of the SR-BI-blocking antibody to cells 1 hr prior to sporozoite addition led to a marked, dose-dependent decrease in infection rate as compared to control samples, measured by the in vitro microscopy-based Huh7 infection assay described above (Figure 2A). Although the blocking antibody used also targets SR-BII (a splicing variant of the same gene), the results from the screen clearly show that knockdown of SR-BII does not lead to any effect on infection (Table S1). This further supports the notion that SR-BI alone accounts for the effects observed in this antibody blocking assay. Similar dose-dependent decreases in *P. berghei* sporozoite infection rates were observed when cells were similarly incubated with BLT-1, BLT-2, or BLT-4 throughout the 24 hr infection period, showing IC_{50} values of 0.9, 5.2, and 19.9 μM, respectively (Figures 2B–2D). Importantly, incubation of the cells with the isostructural, but essentially inactive, semicarbazone derivative of BLT-1 (BLT-1sc), recently shown to be ineffective in inhibiting SR-BI (Nieland et al., 2008), had no effect on infection (Figure 2E), lending further support to SR-BI's role in these infection assays. As can be expected from the quite distinct assays and experimental system used here, these values differ from the multiple corresponding IC_{50} measurements published previously for these compounds, looking at various other activities (Nieland et al., 2002). It is nonetheless notable that the relative efficiencies with which the different BLT compounds inhibited sporozoite infection closely mirror their previously reported effects on the selective uptake of lipids, with BLT-1 being two to five times and

20–38 times more efficient than BLT-2 and BLT-4, respectively, thus suggesting a possible structural link between the two activities. Importantly, infection rates were not affected by preincubation of *Plasmodium* sporozoites with BLT-1 for 1 hr prior to addition to cells, showing that BLT-1 has no effect on sporozoite viability (data not shown).

In sum, although we fully expect that each of the different reagents used here carry different specificity ''footprints,'' the high reproducibility of the observed phenotypes in our assays using multiple distinct siRNAs, several synthetic compound inhibitors, and a blocking antibody clearly support a causality linked to the single target common to all of these, i.e., SR-BI. Thus, altogether, the results strongly indicate a clear role for SR-BI during *P. berghei* sporozoite infection of Huh7 cells.

SR-BI Plays a Role in *P. berghei* In Vivo Infection and in *P. falciparum* Infection of Human Primary Hepatocytes

Because the above experiments were all performed in vitro with the human hepatoma cell line Huh7, we sought to validate the role of SR-BI in *Plasmodium* infection under more physiologically relevant conditions. To this end, we first confirmed that inhibition of SR-BI also leads to a reduction in *P. berghei* infection of primary mouse hepatocytes (Figure S2, $p < 0.001$).

Next, we also confirmed the relevance of these findings in vivo, using systemically delivered, liposome-formulated siRNAs to silence SR-BI expression in adult mice and subjecting these to infection by *P. berghei* sporozoites. Here, we used a qRT-PCR-based assay to quantify infection rates by measuring levels of *Plasmodium* 18S RNA found within extracts of liver samples harvested 40 hr after intravenous (i.v.) sporozoite injection. As for all RNAi analyses, the gene specificity of RNAi-induced phenotypes was extensively controlled in the present in vivo experiments. This first included the parallel treatment of mice with a negative control ''nontargeting'' siRNA (targeting a transcript that is not expressed in these mice, in this case luciferase) to detect sequence-independent off-target effects. Sequence-dependent off-target effects were addressed by testing of multiple distinct siRNA sequences targeting *SR-BI*.

In vivo RNAi treatments have previously yielded potent gene-specific knockdowns in rodent livers with stable lipid nanoparticles (Akinc et al., 2008). In our experiments, SR-BI expression was also reduced successfully in adult mouse livers with three distinct *SR-BI*-specific siRNAs, each of which yielded ~25%–45% remaining *SR-BI* mRNA, as measured by qRT-PCR of tissue extracts taken 76 hr after a single i.v. injection and normalization to *SR-BI* mRNA levels in the livers of adult mice treated with control siRNA (Figure 3A, $p < 0.001$, gray bars). This silencing was also confirmed at the protein level by semiquantitative western blotting of corresponding liver extracts (Figure S3, $p < 0.01$) and at the physiological level by confirmation of the increased blood cholesterol level that is expected from lowered SR-BI function (Figure S4).

Compared to control siRNA treatments, this administration of different *SR-BI*-specific siRNAs resulted in a significant reduction of liver infection by *P. berghei* sporozoites, yielding 30%–50% of control infection loads, as measured by qRT-PCR of *P. berghei* 18S rRNA in samples taken 40 hr after sporozoite injection (Figure 3A, $p < 0.001$, black bars). In a parallel experiment, mice treated with one of the *SR-BI* siRNAs also showed a reduction in the number of parasites reaching the bloodstream, compared to their controls (Figure 3B, $p < 0.05$). Although by day 4 after sporozoite injection, all mice in the control group were positive for blood stages, only two out of five mice were positive in the group pretreated with *SR-BI* siRNA (Figure 3B).

As further confirmation that the observed effects on infection were due to SR-BI loss of function and were not indirect consequences of unspecific toxicities possibly triggered by the siRNA treatments, extensive analyses of tissue and serum markers for activation of the interferon response pathway and a broad range of toxicities clearly showed that the present *SR-BI* siRNA treatments did not cause any pronounced effects of these types, and any reproducible individual changes failed to correlate with our *Plasmodium* infection results (Figures S5, S6, and S7). Finally, it is also noted that the siRNA formulation and delivery methodology used here was recently shown to yield no detectible disruption of the endogenous microRNA pathway (John et al., 2007).

Next, we sought to test the strong prediction from the above data that transgenic mice engineered to be SR-BI-deficient should also show decreased liver infection rates. The results from such mice required careful analysis because homozygous *SR-BI*$^{-/-}$ mice have recently been shown to exhibit clear signs of oxidative stress, including elevated expression of several genes such as heme oxigenase 1 (*HO-1*) (Van Eck et al., 2007). Interestingly, we have recently shown that HO-1 plays a key role in malaria-associated pathology during the blood stages of infection (Pamplona et al., 2007). More directly relevant for the present study, we have also found that as little as a 2-fold overexpression of HO-1 in mouse liver in vivo can lead to an 8-fold increase in liver infection by *P. berghei* sporozoites (Epiphanio et al., 2008). This study shows that HO-1 overexpression blocks the inflammatory response normally mounted against the liver stage of infection, thus yielding a more permissive environment for the parasite. In our hands, homozygous *SR-BI*$^{-/-}$ mice indeed displayed liver *HO-1* mRNA levels approximately 10-fold (range of 3-fold to 20-fold) higher than those of wild-type mice, consistent with the observations of Van Eck et al., and heterozygous *SR-BI*$^{+/-}$ mice showed no significant increase in HO-1 levels compared to wild-type *SR-BI*$^{+/+}$ mice (Figure 3C, $p < 0.001$). As such, this would be expected to increase infection rates vastly in homozygous *SR-BI*$^{-/-}$ mice, thus likely counteracting or masking the predicted negative effects of SR-BI deficiency. Interestingly, we observed significantly decreased *P. berghei* infection rates in heterozygous *SR-BI*$^{+/-}$ mice (Figures 3D and 3E, $p < 0.001$), whose HO-1 levels are similar to those of wild-type *SR-BI*$^{+/+}$ mice, whereas homozygous *SR-BI*$^{-/-}$ mice, whose HO-1 expression levels are greatly increased, showed infection levels comparable to those of wild-type mice (Figure 3D). This demonstrates that the SR-BI-related impairment of infection was potent enough to fully counteract for the significant increase in HO-1 expression in *SR-BI*$^{-/-}$ mice. This observation was also supported by results from mice deficient for PDZK1, which are also known to exhibit nearly null levels of hepatic SR-BI (Kocher et al., 2003). Like the *SR-BI*$^{-/-}$ mice, *PDZK1*$^{-/-}$ mice also showed infection levels comparable to those of controls, despite also having the elevated HO-1 expression expected to yield significantly increased infection (Figure S8, $p < 0.05$). Nevertheless, this does not rule out the possibility that other unknown factors,

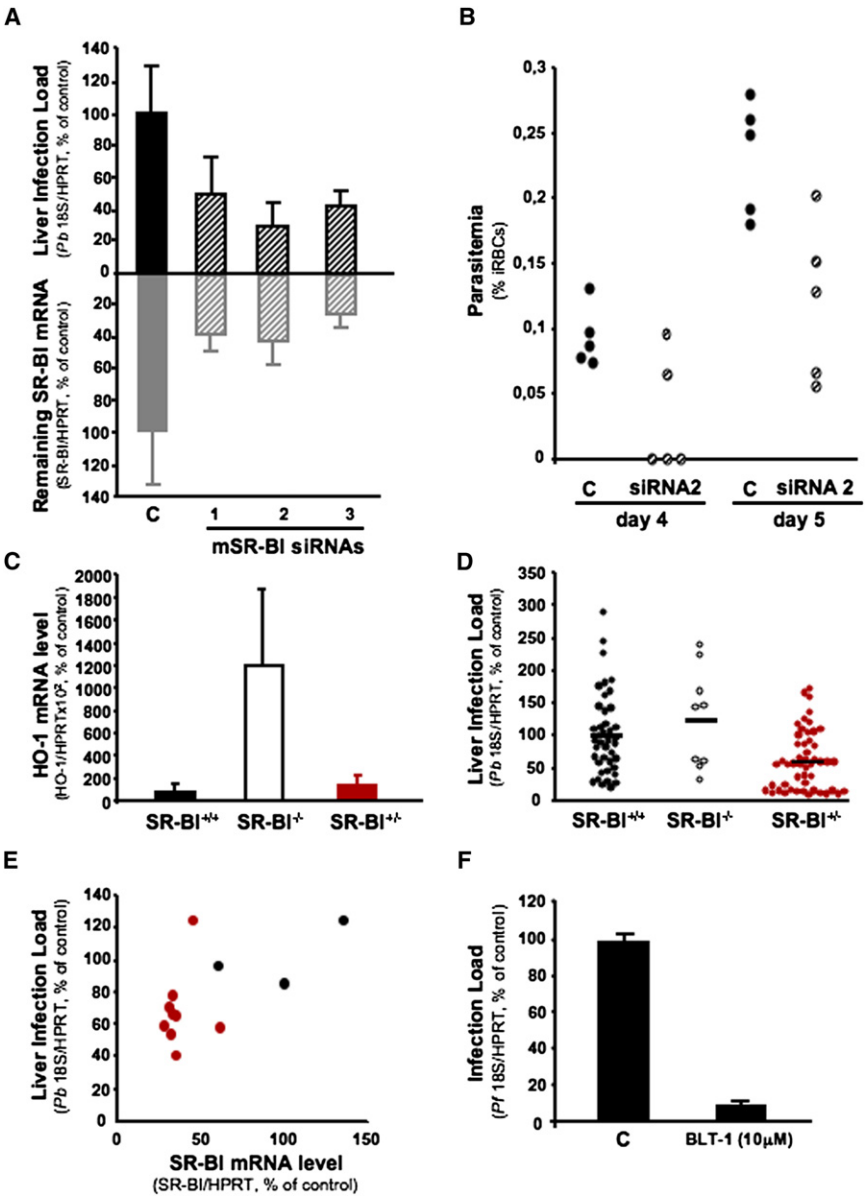

Figure 3. Host SR-BI Plays a Key Role in *P. berghei* Infection In Vivo

(A and B) Effect of siRNA-mediated in vivo knockdown of SR-BI on mouse liver stage (A) and blood stage (B) infection by *P. berghei.* Liver infection load ([A], black bars) was measured by qRT-PCR analysis of *P. berghei* 18S rRNA normalized to hypoxanthine-guanine phosphoribosyltransferase (HPRT) in liver extracts taken 40 hr after sporozoite i.v. injection, and plotted as percentage of the mean of negative control samples ("C"). Grey bars in (A) represent the remaining mRNA levels for the targeted m*SR-BI* gene in the same liver samples. Results are expressed as the mean ± SD of five mice per group. Effect on blood stage of treatment of one *SR-BI* siRNA (B) was measured by parasitemia (percentage of infected red blood cells, iRBC) quantification with FACS. Mice treated with a siRNA targeting luciferase were used as control. Although all mice were positive in the control group by day 4 after sporozoite infection, only two out of five mice were positive in the group treated with *SR-BI* siRNA at day 4. All mice became positive by day 5.

(C) *HO-1* mRNA levels were measured in the livers of infected *SR-BI*$^{-/-}$, *SR-BI*$^{+/-}$, and wild-type (*SR-BI*$^{+/+}$) mice, collected 40 hr after sporozoite i.v. injection. Results are expressed as the mean ± SD of the results obtained for 12 wild-type (*SR-BI*$^{+/+}$), four *SR-BI*$^{-/-}$, and nine *SR-BI*$^{+/-}$ mice.

(D and E) Level of liver *P. berghei* in vivo infection was determined in SR-BI-deficient mice (D) by qRT-PCR analysis of *P. berghei* 18S rRNA normalized to HPRT in liver extracts taken 40 hr after sporozoite i.v. injection and plotted as percentage of the mean of control SR-BI wild-type mice (*SR-BI*$^{+/+}$). SR-BI wild-type (*SR-BI*$^{+/+}$, n = 42), homozygous (*SR-BI*$^{-/-}$, n = 9), and heterozygous (*SR-BI*$^{+/-}$, n = 50) SR-BI-deficient mice are represented in black, white, and red circles, respectively. Black bars represent the average of the infection level in each experimental group. Comparison of the infection rate versus *SR-BI* mRNA level in *SR-BI*$^{+/+}$ and *SR-BI*$^{+/-}$ mice (in black and red circles, respectively), measured by qRT-PCR, shows a correlation between the infection rate and the level of SR-BI expression in the liver (E).

(F) Host SR-BI plays a key role in infection of primary human hepatocytes by *P. falciparum.* Effect of BLT-1 on *P. falciparum* infection in human primary hepatocytes was measured by qRT-PCR. BLT-1 was added to cells 1 hr before sporozoite addition, and infection load was measured in cell extracts taken 72 hr after sporozoite addition, as described in the main text. Results are expressed as the mean ± SD of triplicate samples.

deregulated in *SR-BI*$^{-/-}$ mice, could also contribute to the infection levels observed in these mice. Finally, the significantly altered, pathological physiology of *SR-BI*$^{-/-}$ mice may also include long-term compensatory survival adaptations that provide the parasite with alternative infection paths. Altogether, these results unambiguously confirm the RNAi-based observations that SR-BI indeed plays an important role in the liver stage of *Plasmodium* infection in vivo.

Finally, we note that all of the above experiments were carried out with *P. berghei*, whose natural preference for rodent hosts entails the possibility that its infection strategy may differ in certain respects from that of human-pathogenic *Plasmodium* species such as *P. falciparum*. The role of SR-BI was therefore also tested for *P. falciparum* infection in human primary hepatocytes 72 hr after sporozoite addition, with the same qRT-PCR-based assay of *Plasmodium* 18S RNA used above. Once again, BLT-1 treatment of human primary hepatocytes caused a significant and specific decrease of *P. falciparum* infection in these cells (Figure 3F, $p < 0.001$). Altogether, these data unequivocally confirm the important role of host SR-BI expression in the liver stage of *Plasmodium* infection not only in vitro but also in vivo, and not only for the rodent malaria parasite, *P. berghei*, but also for *P. falciparum*, the deadliest of human malarial pathogens.

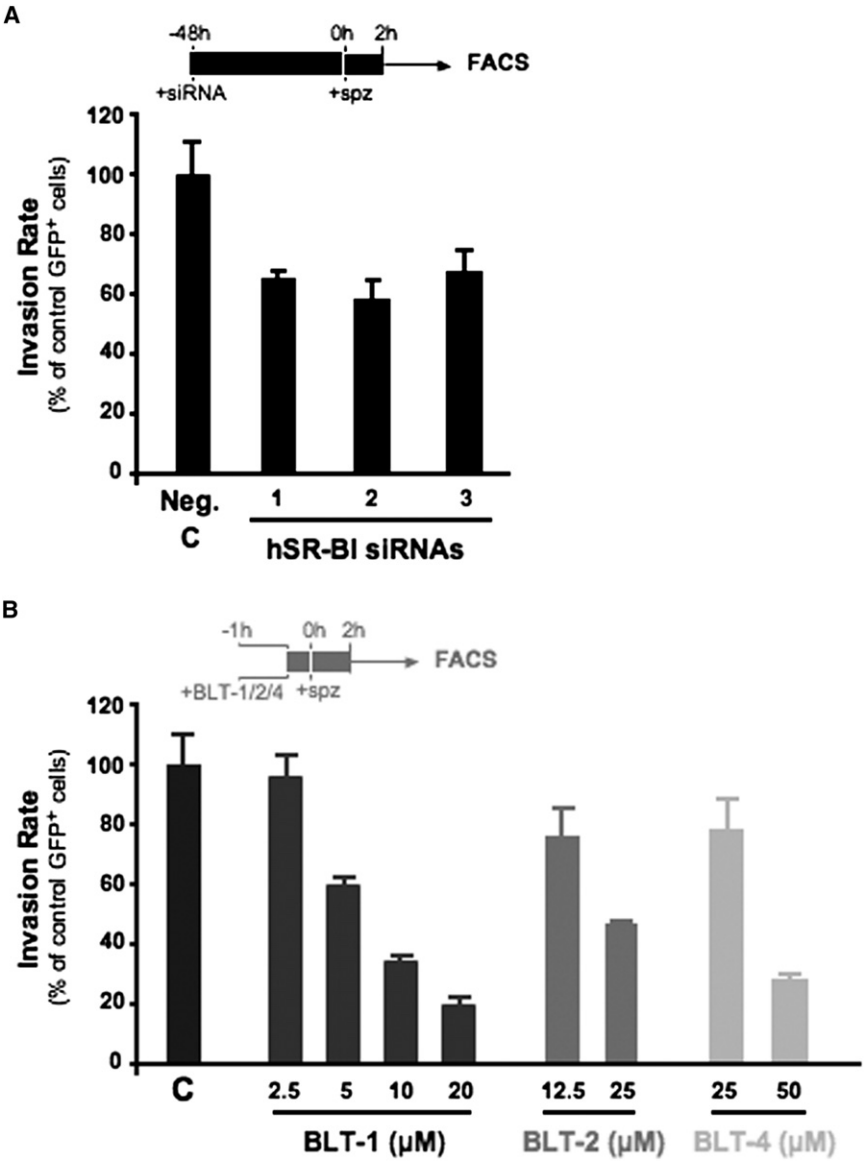

Figure 4. Host SR-BI Plays a Role in Invasion of *P. berghei* in Huh7 Cells

(A and B) FACS analysis of effects of siRNA-mediated knockdown of SR-BI (black bars) or different concentrations of BLT-1, BLT-2, and BLT-4 treatment (gray bars) on invasion phase of infection in Huh7 cells, with GFP-expressing *P. berghei* sporozoites. As indicated in diagrams above the bar charts, cells were harvested for flow cytometry 2 hr after sporozoite addition, and invasion rate was measured as percentage of GFP^+ cells compared to control values. For siRNA-treated samples, control samples (Neg. C) were treated with a nonspecific siRNA. For BLT-treated samples, control (DMSO) was treated with drug dilution buffer containing same level of DMSO found in the most concentrated drug treatment. Results are expressed as the mean ± SD of triplicate samples.

Host Cell SR-BI Is Involved in Both Invasion and Development of *Plasmodium* inside the Parasitophorous Vacuole

Having established the basic effects of SR-BI inhibition on liver infection both in vitro and in vivo, we next sought to gain further mechanistic insights by dissecting the infection process into its constituent steps. Hepatocyte infection by *Plasmodium* can be conceptually viewed as comprising three consecutive steps: cell traversal, productive hepatocyte invasion, and intracellular development. Since our in vitro infection model enables us to distinguish between these steps, we aimed to determine which of these involved SR-BI function.

Over 95% of the infective sporozoites in our standard in vitro assay described above have completed the traversal and invasion steps at 2 hr after addition to the cells (Prudencio et al., 2008). In order to quantify traversed versus invaded cells prior to EEF development most accurately, we used a fluorescence-activated cell sorting (FACS)-based assay (Prudencio et al., 2008). In brief, Huh7 cells were infected with GFP-expressing *P. berghei* sporozoites in the presence of rhodamine-dextran. Two hours after sporozoite addition, cells were harvested and analyzed by FACS. Cells that had been transiently traversed by sporozoites were identified as rhodamine-dextran positive, whereas cells successfully invaded by sporozoites were identified by the presence of GFP and the absence of rhodamine-dextran (Mota et al., 2001) (Figure S9). Pretreatments of the host cells with three distinct *SR-BI*-targeting siRNAs, as characterized above, did not lead to any difference in the number of traversed cells (Figure S9). Still, these treatments yielded significant reductions in the proportion of Huh7 cells invaded by *P. berghei* sporozoites, as compared to controls (Figure 4A, $p < 0.001$). Similarly, treatment with BLT-1, BLT-2, or BLT-4 also led to a dose-dependent decrease in invaded cells measured 2 hr after sporozoite addition (Figure 4B). These results unambiguously reveal a key role for SR-BI during the initial invasion step of sporozoite infection.

We next examined whether SR-BI also has a role in the following step of sporozoite infection, i.e., development of the EEF within the parasitophorous vacuole. Pretreatments of the Huh7 cells with *SR-BI*-specific siRNAs, or exposure to blocking antibody or small molecule inhibitors (BLTs) throughout the full 24 hr infection period of our in vitro microscopy assay all yielded marked decreases in EEF size, as measured with automated image analysis algorithms (Figures 5A and 5B). The absence of larger EEF size classes noted with this analysis suggested a possible blockage of EEF development. Detailed FACS analysis of Huh7 cells infected with GFP-expressing *P. berghei* also revealed this effect of BLT-1, BLT-2, and BLT-4 treatment on

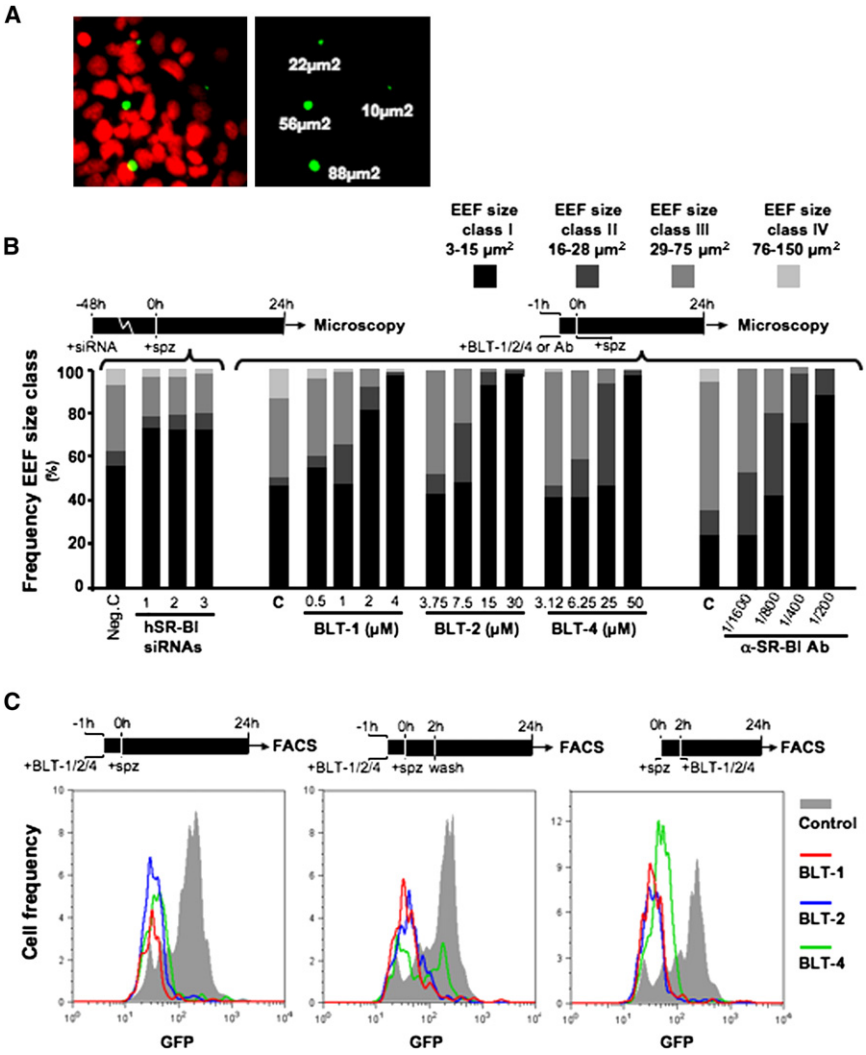

Figure 5. Host SR-BI Plays a Role in Development of *P. berghei* in Huh7 Cells

(A) Representative pictures of EEFs in cells fixed 24 hr after sporozoite addition. Cell nuclei are represented in red and EEFs in green. Automated analysis of microscopy images enabled the classification of EEFs in four size classes defined within the area ranges detailed in the grayscale color code shown.

(B) Effect of siRNA-mediated knockdown of SR-BI and different concentrations of BLT-1, BLT-2, and BLT-4 treatment, as well as serial dilutions of a SR-BI-blocking antibody on *P. berghei* development within host Huh7 cells, as determined by EEF size classification via automated analysis of microscopy images from cells fixed 24 hr after sporozoite addition. Data shown are from the samples used for infection rate analysis in Figure 2. Four classes of EEF sizes are represented as different gray levels used in bar fills, ranging from black for EEFs with the smallest areas, up to lightest gray tone for the largest EEFs. For siRNA-treated samples, control samples (Neg. C) were treated with a nonspecific siRNA. For BLT-treated samples, control samples ("C") were treated with drug dilution buffer containing same level of DMSO found in most concentrated drug treatment. For samples treated with SR-BI-blocking antibody, control samples were exposed to antibody dilution buffer containing same azide concentration present in most concentrated antibody treatment. As indicated in diagram above bar chart, cells were either treated with siRNAs 48 hr before sporozoite addition or treated with the different BLT inhibitors and the antibody 1 hr before sporozoite addition. Results are expressed as the mean of triplicate samples.

(C) Effect of BLT-1, BLT-2, and BLT-4 treatment on *P. berghei* development within host Huh7 cells, as measured by FACS in cells harvested at 24 hr after addition of GFP-expressing sporozoites. Control represents cells treated with drug dilution buffer containing same level of DMSO found in drug treatment. Drug incubation periods are indicated in the diagrams above the charts. The graphs display representative datasets of triplicate experimental samples.

EEF development. This analysis showed that, in addition to the marked decrease in number of infected cells already noted 2 hr after sporozoite addition (Figure 4B), a significant decrease in GFP intensity becomes apparent within the infected cells at the 24 hr or 48 hr time points (Figure 5C, Figures S10 and S11). Altogether, these results are consistent with a defect in *P. berghei* development as a result of SR-BI inhibition.

However, since invasion was also affected under the above assay conditions, we conducted more precise tests to address the development stage more unambiguously. We investigated whether BLT-1, BLT-2, and BLT-4 retain their inhibitory effect on infection when added only after completion of sporozoite invasion, *i.e.*, 2 hr after sporozoite addition to cells under our assay conditions. When infection was measured 24 hr after sporozoite addition, treated cells showed a drop in GFP intensity relative to controls comparable to that observed after 24 hr exposure to similar amounts of the same compounds (Figure 5C). This drop was even more notable when infection was assessed 48 hr after sporozoite addition (Figure S11). In a parallel experiment, samples were incubated with BLT-1, BLT-2, and BLT-4 for the first 2 hr after sporozoite addition and subsequently washed with fresh medium. Infection was then measured by FACS 24 hr or 48 hr later. The results show that this treatment led not only to the expected decrease in the proportion of infected cells due to a reduced invasion but also to a drop in GFP intensity (Figure 5C and Figure S11). Together, these data indicate that host liver cell SR-BI function is required not only for sporozoite invasion but also for the subsequent development of EEFs within the parasitophorous vacuole.

Next we aimed to gain mechanistic insights into the functional contributions of SR-BI in both these steps of infection. With regard to SR-BI's observed role in the invasion step, one could envisage that SR-BI might be fulfilling at least some receptor-like functions for the sporozoite, mediating its initial binding

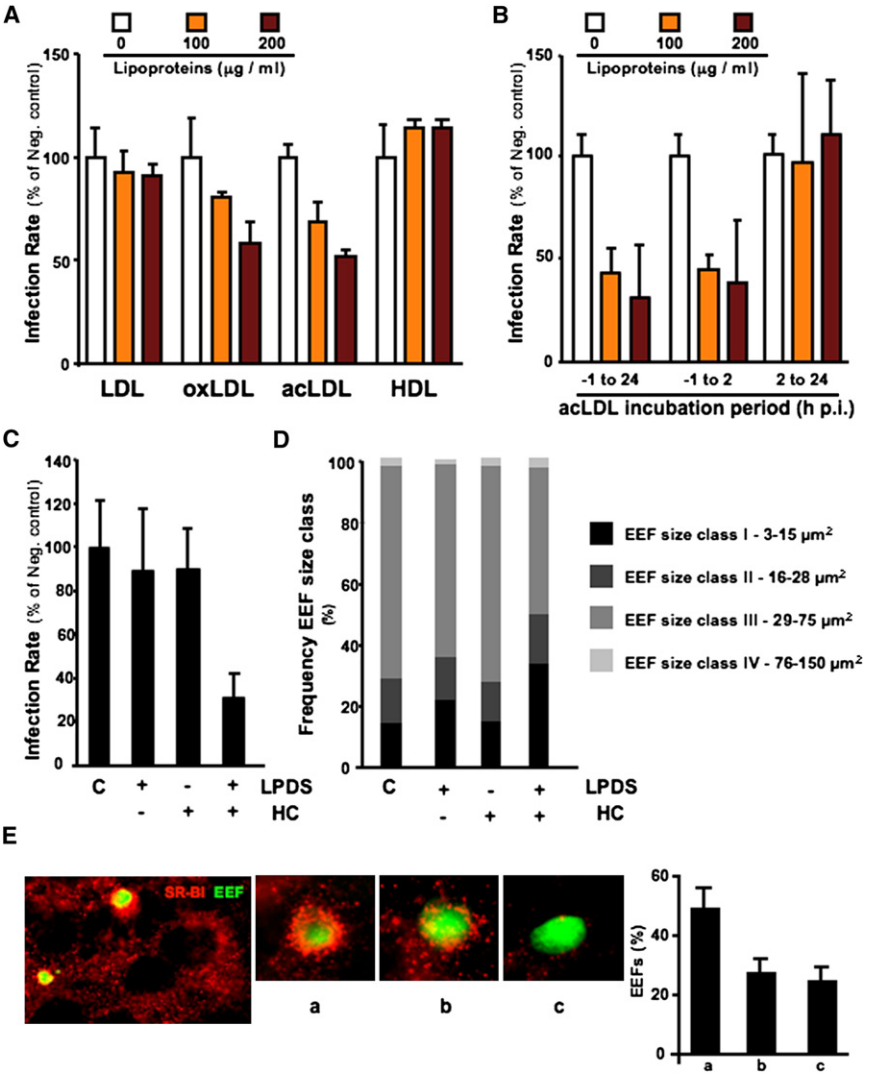

Figure 6. Mechanistic Insights into SR-BI Roles in Infection

(A) Effect of different concentrations of LDL, acLDL, oxLDL, and HDL on Huh7 cell infection by *P. berghei* sporozoites. Results are expressed as the mean ± SD of three independent infections.

(B) Quantification of infection of Huh7 cells incubated with acLDL at various time points relative to addition of *P. berghei* sporozoites. All infections were measured 24 hr after sporozoite addition. Results are expressed as the mean ± SD of three independent infections.

(C) Effect of cholesterol depletion on Huh7 cell infection by *P. berghei* sporozoites. LPDS, lipoprotein-deficient serum; HC, hydroxycholesterol. Control cells ("C") were grown and infected in the complete medium and in the absence of HC. Results are expressed as the mean ± SD of three independent infections.

(D) Effect of cholesterol depletion on *P. berghei* development within host Huh7 cells, as determined by EEF size classification via automated analysis of microscopy images from cells fixed 24 hr after sporozoite addition. Data shown are from the samples used for infection rate analysis in (C). Four classes of EEF sizes are represented as different gray levels used in bar fills, ranging from black for EEFs with the smallest areas up to lightest gray tone for the largest EEFs. Control cells ("C") were grown and infected in the complete medium and in the absence of HC.

(E) Immunofluorescence analysis of SR-BI localization in infected Huh7 cells fixed 24 hr after addition of *P. berghei* sporozoites. The plot represents the quantification of the percentage of EEFs (green) with different levels of SR-BI (red) in immediate proximity, according to classification shown in small images: a, high levels of SR-BI staining in the proximity of the EEF; b, medium levels of SR-BI staining in the proximity of the EEF; and c, no SR-BI staining in the proximity of the EEF. Results are expressed as the mean ± SD of EEFs (%) in three independent infections.

and entry into the cell either directly or indirectly, through associated cholesterol or lipoprotein particles. To test these hypotheses, we infected cultured human Huh7 hepatoma cells grown in medium containing lipoprotein-deficient serum (LPDS) with isolated *P. berghei* sporozoites in the presence of defined amounts of human lipoproteins know to bind to SR-BI, namely high-density lipoprotein (HDL), low-density lipoprotein (LDL), acetylated LDL (acLDL), or oxidized LDL (oxLDL). Infection rates were then quantified by fluorescence microscopy. Both modified forms of LDL (modLDL) reproducibly reduced the infection levels ($p < 0.01$ and $p < 0.001$ for concentrations equal or higher than 100 μg/ml of oxLDL and acLDL, respectively), whereas LDL or HDL did not (Figure 6A). The expected inhibition of infection was only observed when the added acLDL or oxLDL were present during the first 2 hr after sporozoite addition to the cells, i.e., the invasion phase (Figure 6B, $p < 0.001$). These results strongly suggest that elevated levels of exogenous modLDL reduce *Plasmodium* infection of hepatoma cells primarily by inhibiting the sporozoite invasion step. In addition, it also clearly shows that none of the lipoproteins tested facilitate sporozoite entry, making it unlikely that these lipoprotein particles play a bridging or "carrier" role for the invading sporozoites. In fact, our data suggest that if SR-BI indeed acts as a receptor or coreceptor for sporozoite invasion, it most likely does so through direct interactions with the sporozoite, which are apparently susceptible to competitive inhibition from modLDL. Nevertheless, the possibility also exists that other receptors for modLDL may be present in the vicinity of SR-BI, thereby influencing SR-BI-mediated parasite invasion. These possibilities clearly warrant further analysis.

Beyond the invasion step, our results also show that SR-BI plays an important role in EEF development. Inside hepatocytes, *Plasmodium* sporozoites undergo a major transformation, with each giving rise to thousands of merozoites, necessarily requiring the availability of sufficient lipids for the synthesis of large amounts of new membranes. It is therefore tempting to hypothesize that our observations may reflect a direct involvement of the host cell SR-BI's selective lipid uptake activity in "feeding" cholesteryl esters and other lipids to the parasite across the parasitophorous vacuole membrane. Thus, we sought to determine the parasite requirements for lipids from extracellular and

intracellular sources. To this end, infections with *P. berghei* sporozoites were assayed in Huh7 hepatoma cells depleted of external lipids via growth in LPDS medium, depleted of internal lipid sources via hydroxycholesterol (HC) treatment, or depleted of both by combining the two conditions. The results clearly show that Huh7 infection by *P. berghei* sporozoites is significantly reduced only when both internal and external sources of lipids are depleted, as shown by the quantification of EEF numbers by microscopy (Figure 6C), as well as EEF size reductions (Figure 6D). Importantly, SR-BI staining can be observed in the periphery of the parasitophorous vacuole of 79.5% ± 6.3% of intracellular EEFs (Figure 6E), thus supporting roles at both the cytoplasmic membrane as well as within the intracellular environment to the developing EEF.

Host Cell SR-BI Constitutes a Natural Limiting Factor for *Plasmodium* Sporozoite Infection

All the above results implicate SR-BI as an important factor for both *Plasmodium* sporozoite invasion and EEF development inside host liver cells. It was therefore of clear interest to determine in what capacity SR-BI might also represent a natural limiting factor for infection. We tested this hypothesis by examining whether transient overexpression of SR-BI could lead to an increase in invasion and/or infection in cells such as HeLa that are normally less permissive than Huh7 to *Plasmodium* sporozoites. The same test was also carried out in Huh7 cells to determine in parallel whether their wild-type levels of SR-BI represent a natural rate-limiting step for their own infectability. To this end, Huh7 and HeLa cells, the latter of which normally express much lower levels of SR-BI (as confirmed here in Figures 7A and 7B), were transfected with a CMV promoter-driven, *SR-BI*-expressing plasmid and subjected to our *P. berghei* infection and invasion assays as described above. The results clearly show that our transient transfection yields the expected significant increase in SR-BI expression in both Huh7 and HeLa cells, as detected both at mRNA (Figure 7A) and protein levels (Figure 7B). In addition, SR-BI-specific extracellular staining also shows that a significant proportion of cells express SR-BI at their surface (Figure 7C), consistent with the protein's expected functionality. Importantly, significant increases in *P. berghei* sporozoite infection and invasion correlated clearly with SR-BI expression rise (Figures 7D and 7E and Figure S12, $p < 0.01$). Moreover, inhibition of SR-BI function with a synthetic inhibitor in overexpressing cells causes infection rates to revert back down to levels comparable to those of control cells treated with the same inhibitor (Figure S12). Thus, taken together, these data add yet further support and confirmation for the functional role of host SR-BI in sporozoite infection, demonstrating that SR-BI function represents a natural limiting factor controlling the susceptibility of otherwise refractory cells to *Plasmodium* infection.

DISCUSSION

The present study adds significant new insights into the host molecules and cellular processes underlying this parasite's infection of the liver. In particular, our results confirm and extend earlier suggested links between liver infection and lipoprotein pathways (Shakibaei and Frevert, 1996; Sinnis et al., 1996). By using several types of inhibitors including RNAi both in vitro in cultured human cells and in vivo in a mouse model of infection, we have identified a major lipoprotein receptor, SR-BI, as a functionally important host factor for both sporozoite invasion and EEF development. SR-BI is a 509-amino acid, 82 kDa glycoprotein, with two cytoplasmic C- and N-terminal domains separated by a large extracellular domain. It mediates the traffic of cholesterol to and from lipoproteins, acting as the major receptor for HDL, but also handling acLDL, oxLDL, and native LDL. SR-BI expression is highest in tissues with critical roles in cholesterol metabolism and is also expressed in a series of cell lines maintained in culture (reviewed in Rhainds et al., 2003).

Our present data support the conclusion that SR-BI defines a preferred path, though not necessarily the only one, for liver infection by *Plasmodium* sporozoites. Indeed, the possibility of other alternative, SR-BI-independent paths is formally suggested by our observation that infection is still detectable in SR-BI null mice, although the relevance of this result to less extreme physiological contexts remains unclear. It is also notable that *P. berghei* is more promiscuous than *P. falciparum* and has been shown to use alternative pathways of invasion depending on the cell type (Silvie et al., 2007). Regardless, our findings of increased infection after SR-BI overexpression in both Huh7 and the normally nonpermissive HeLa further suggest that SR-BI represents a strongly enabling and naturally limiting factor for *Plasmodium* infection.

Our data also offer some mechanistic characterization of SR-BI's contributions to individual steps of the liver infection process, revealing detectable roles in both the productive invasion of host hepatocytes by sporozoites and in development of the resulting EEFs. By placing these observations in the context of SR-BI's known functions in lipid transport, we have tested several hypotheses that might account for SR-BI's role in infection. First, with regard to SR-BI's observed role in the invasion step, we have hypothesized that SR-BI might mediate the sporozoite's initial binding and entry into the cell either directly or indirectly, through associated cholesterol or lipoprotein particles. Our results allow us to exclude the latter possibility, as addition of lipoproteins known to bind SR-BI either has no effect or leads to a decrease rather than an increase in invasion. Thus, our data suggest that if SR-BI indeed acts as a receptor or coreceptor during invasion, it likely does so through direct interaction with the parasite in a manner that is vulnerable to competition from modLDL forms but not from HDL. This is interesting from the point of view that SR-BI domains involved in interactions with HDL and modLDL forms have been shown to be separable (Gu et al., 2000). The alternative possibility also remains that effective sporozoite invasion requires a very specific balance in the host cell plasma membrane's lipid composition, which itself is directly dependent upon SR-BI activity. Further in depth testing is underway to distinguish between these possibilities.

Beyond the invasion step, our results also show that SR-BI plays an important role in EEF development. Inside hepatocytes, *Plasmodium* sporozoites undergo a major transformation, with each giving rise to thousands of merozoites. However, the sporozoite's requirements and the strategies it has developed to survive and to be successful remain poorly understood (reviewed in Prudencio et al., 2006). Regardless, the parasite's extensive proliferation during this stage necessarily requires the availability of sufficient lipids for the synthesis of large amounts of additional membranes. It is therefore tempting to hypothesize

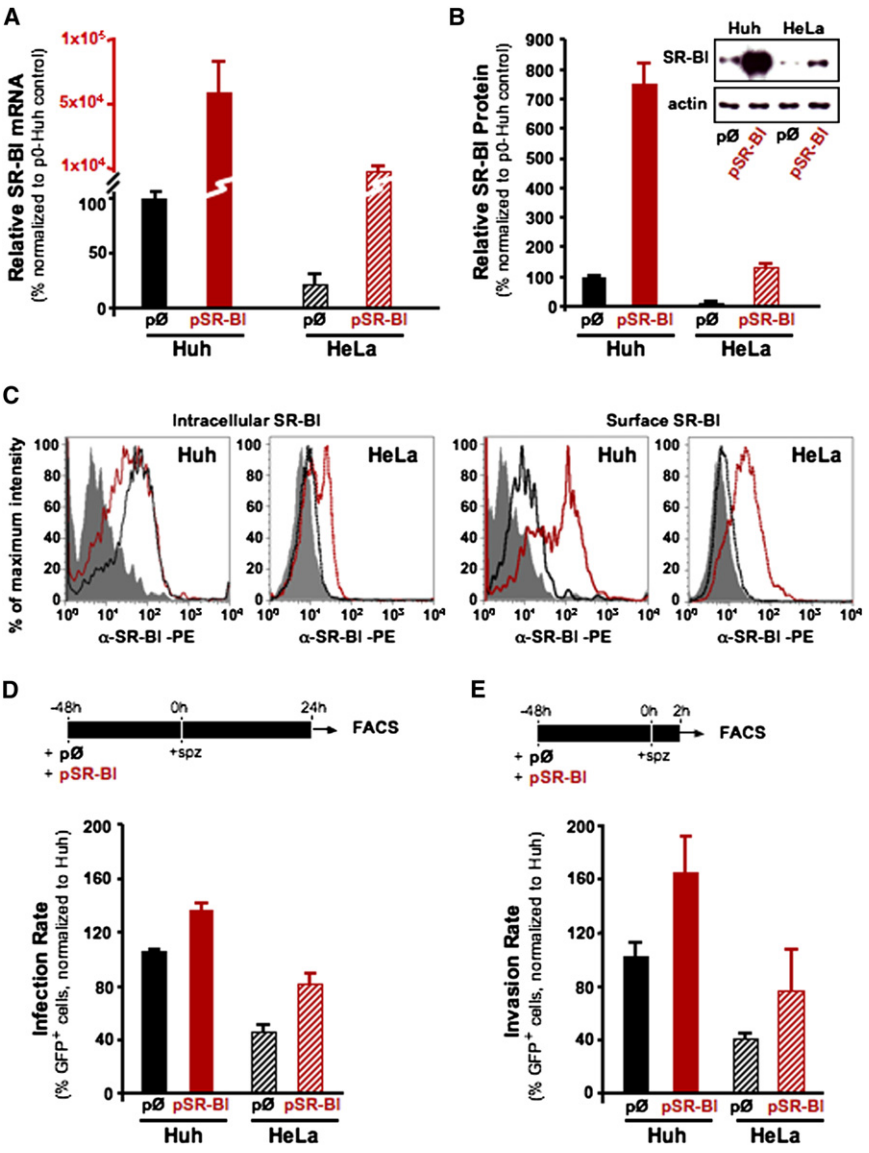

Figure 7. Overexpression Studies Reveal that Host SR-BI Plays a Role in Both Invasion and Development of *P. berghei* in Permissive and Less-Permissive Cell Lines

(A and B) Effect of *SR-BI* overexpression on SR-BI mRNA (A) and protein (B) levels in Huh7 and HeLa cells, measured, respectively, by qRT-PCR and semiquantitative western blotting of cell extracts collected 48 hr after cell transfection from cells transfected with a plasmid with the *SR-BI* gene cloned (pSR-BI, in red) or with the same empty plasmid (pØ, in black). Results are expressed as the mean of triplicate samples ± SD and were normalized to the control pØ of Huh7 cells (100%).

(C) Effect of SR-BI overexpression on intracellular and surface SR-BI protein levels in Huh7 and HeLa cells, measured by flow cytometry. The black and red lines correspond to cells transfected with pØ and pSR-BI and stained with an anti-SR-BI antibody labeled with phycoerythrin (α-SR-BI-PE), whereas the gray area represents the negative control of pØ unstained cells.

(D) Effect of SR-BI overexpression on Huh7 and HeLa cells infection by GFP-expressing *P. berghei* sporozoites, measured 24 hr after sporozoite addition by flow cytometry. Bar code colors are the same as above. Results are expressed as the mean of triplicate samples ± SD and were normalized to the control pØ of Huh7 cells (100%).

(E) Effect of SR-BI overexpression on invasion of GFP-expressing *P. berghei* sporozoites within Huh7 and HeLa cells, measured 2 hr after sporozoite addition by flow cytometry. Bar and line colors are the same as above. Results are expressed as the mean of triplicate samples ± SD and were normalized to the control pØ of Huh7 cells (100%).

that our observations may reflect a direct involvement of the host cell SR-BI's selective lipid uptake activity in "feeding" cholesteryl esters and other lipids to the parasite. Our data show that the depletion of all sources of cholesterol reduces infection, including EEF development, whereas the complete absence of extracellular cholesterol alone, in form of lipoproteins, has no direct impact on the latter. These observations indeed suggest that SR-BI's role in EEF development may result from its activity in lipid transfer and that the intracellular stores of cholesterol, more so than extracellular lipoproteins, are the source of the transferred cholesterol. Interestingly, immunofluorescence staining of infected cells reveals an accumulation of SR-BI in the proximal periphery of intracellular EEFs, supporting a possible role of this molecule in providing cholesterol to the developing parasites. Nevertheless, one should also consider the possibility that the SR-BI effect may not necessarily be due to a direct transport of cholesterol to the parasite but may instead result from other roles of lipids on membrane organization and signaling. Although our results provide important evidence for possible mechanisms underlying the observed effects of SR-BI in *Plasmodium* infection, more detailed analyses will be required to further test the validity of the different hypotheses.

Finally, it should be noted that, although the physiological complications observed in the extreme context of the homozygous *SR-BI*$^{-/-}$ mice may warrant some caution in considering sustained, long-term treatments of patients with SR-BI inhibitors, such real-world pharmacological applications rarely come close to achieving 100% loss of function of their target and are therefore most likely to resemble the more benign physiology observed in heterozygous *SR-BI*$^{+/-}$ mice and siRNA-treated mice. Thus, the present study establishes an important proof of principle for the use of host factors as novel prophylactic or therapeutic drug targets to combat malaria. In fact, targeting host components offers major advantages over targeting the parasite itself, including the inherently lower vulnerability of such drugs, used either alone or in combination therapies, to the development of resistance by the parasite (Cunha-Rodrigues et al., 2006). As a second key advantage, the host factor approach also offers significantly higher potential for accelerated drug discovery and development through synergies with ongoing output from other

disease pipelines. This potential emerges particularly well in the present case of SR-BI, which has recently been proposed to function as a receptor for several pathogens, including hepatitis C virus (HCV) (Scarselli et al., 2002), mycobacteria (Philips et al., 2005), and bacteria (Vishnyakova et al., 2006). Interestingly, it has been proposed that HCV requires functional cooperation between the host's SR-BI and tetraspanin CD81, the latter having also been implicated in *Plasmodium* sporozoite invasion (Silvie et al., 2003, 2007). Thus, our present evidence, implicating host SR-BI in malaria infection, may in fact help to advance our understanding of several other important infectious diseases. By further exploring the parallels between these infection pathways, one can now hope for increasing synergies between all of these fields for years to come.

EXPERIMENTAL PROCEDURES

Cells and Parasites

Huh7 and HeLa cells were cultured, respectively, in supplemented RPMI and Dulbecco's modified Eagle's medium (DMEM). Mouse and human primary hepatocytes were obtained as previously described (Goncalves et al., 2007; Mazier et al., 1985). Green fluorescent protein expressing *P. berghei* (parasite line 259cl2) sporozoites (Franke-Fayard et al., 2004) or *P. falciparum* sporozoites (NF 54 strain) were obtained from dissection of infected female *Anopheles stephensi* mosquito salivary glands.

High-Throughput siRNA Screening of *Plasmodium* Infection

Huh7 cells were transfected 24 hr after being seeded with individual siRNAs, in triplicate, in a final concentration of 100 nM per lipofection. Two days later, cells were infected with *P. berghei* sporozoites and, 24 hr later, cells were fixed and cell nuclei, filamentous actin, and EEFs were stained. Image acquisition and analysis was performed automatically.

Gene-Specific Expression and Infection Quantification by qRT-PCR

For gene-specific expression in vitro, total RNA was isolated from Huh7 cells 48 hr after transfection. Relative amounts of remaining mRNA levels of RNAi targets were calculated against the level of a housekeeping gene. Remaining mRNA levels of RNAi-treated samples were compared with those of samples transfected with negative unspecific siRNA. For infection determination in vivo or ex vivo, total RNA was isolated from livers or primary hepatocytes, respectively. The determination of liver parasite load was performed according to the method developed for *P. yoelii* infections (Bruna-Romero et al., 2001).

Cell Treatment with an Anti-SR-BI Antibody, Chemical Compounds, Lipoproteins, or Hydroxycholesterol

For SR-BI inhibition experiments, cells were incubated with an anti-SR-BI antibody (NB 400-134, Novus Biologicals) or with the chemical compounds BLT-1, BLT-2, BLT-4, or semicarbazone derivative of BLT-1 (BLT-1sc) (ChemBridge). In lipoprotein competition experiments, Huh7 cells were incubated with different concentrations of LDL, oxLDL, acLDL, and HDL (Biomedical Technologies). In cholesterol depletion experiments, Huh7 cells were incubated with 1 μM of hydroxycholesterol.

Fluorescence-Activated Cell Sorting Analysis

FACS analysis at 2, 24, and 48 hr after sporozoite addition was performed as previously described (Prudencio et al., 2008).

In Vivo RNAi

C57Bl/6 mice were treated with a single i.v. administration of 5 mg/kg of siRNA formulated in liposomal nanoparticles (Alnylam), as previously described (Akinc et al., 2008). The sequences of the siRNAs used are shown in Table S2. Thirty-six hours after siRNA administration, mice were infected with *P. berghei* sporozoites. The remaining *SR-BI* mRNA levels and the parasite load in the livers of infected mice were determined by qRT-PCR 40 hr after sporozoite injection, 76 hr after siRNA administration. Interferon response and toxicity effects due to siRNA-treatment of mice were assessed by qRT-PCR or biochemical analysis. SR-BI protein level in the liver was determined by western blot, and the total cholesterol in the serum was determined biochemically.

In Vivo Infection of SR-BI- and PDZK1-Deficient Mice

SR-BI-deficient (*SR-BI*$^{-/-}$ and *SR-BI*$^{-/+}$), *PDZK1*$^{-/-}$, and wild-type mice were infected with 2×10^4 *P. berghei* sporozoites. Parasite load, SR-BI, and *HO-1* mRNA levels in the liver of infected mice were determined by qRT-PCR 40 hr after sporozoite injection. Total cholesterol in serum of infected mice was biochemically determined by DNAtech (INETI, Portugal).

Effect of SR-BI Overexpression in *P. berghei* Infection of Huh7 and HeLa Cells

Huh7 and HeLa cells were transfected in suspension with 1.5 μg of a *SR-BI*-expressing plasmid (pLPCx + SR-BI, Lavie and Dubuisson, Institut Pasteur de Lille, France) with FuGENE 6 (Roche) according to the manufacturer's instructions. As control, cells were transfected with an empty plasmid (pLPCx). Forty-eight hours after transfection, SR-BI overexpression level was measured at the mRNA and protein level by qRT-PCR and western blot, respectively. Intracellular and surface SR-BI was measured by flow cytometry. *P. berghei* infection was determined by flow cytometry at 2, 24, and 48 hr after sporozoite addition.

SUPPLEMENTAL DATA

Supplemental Data include Supplemental Experimental Procedures, 12 figures, and three tables and can be found online at http://www.cellhostandmicrobe.com/cgi/content/full/4/3/271/DC1/.

ACKNOWLEDGMENTS

We thank Sabine Grahl, Luís Santos, Nuno Carmo, Lénia Rodrigues, and Filipa Lopes for technical assistance. We would also like to thank Maria Febbraio for providing the SR-BI homozygous deficient mice, Alina Costa for the breeding of SR-BI heterozygous mice, Jean Dubuisson for providing the SR-BI-expressing plasmid, and Robert Langer and Dan Anderson for generously allowing us to use the lipid formulation for systemic siRNA experiments before its publication. The work was supported by European Science Foundation (EURYI to M.M.M.), Howard Hughes Medical Institute (HHMI), and Fundação para a Ciência e Tecnologia (FCT) of the Portuguese Ministry of Science (grants POCTI/SAU-MMO/60930/2004 and PTDC/BIA-BCM/71920/2006 to M.M.M. and M.P., respectively). C.D.R., M.P., S.P., and S.E. were supported by FCT fellowships (BD/14232/2003, BI/15849/2005, BD/31523/2006, and BPD/31598/2006). M.M.M. is a HHMI International Scholar and a BioMalPar Affiliated Member.

Received: April 11, 2008
Revised: June 27, 2008
Accepted: July 18, 2008
Published: September 10, 2008

REFERENCES

Akinc, A., Zumbuehl, A., Goldberg, M., Leshchiner, E.S., Busini, V., Hossain, N., Bacallado, S.A., Nguyen, D.N., Fuller, J., Alvarez, R., et al. (2008). A combinatorial library of lipid-like materials for delivery of RNAi therapeutics. Nat. Biotechnol. *26*, 561–569.

Alonso, P.L., Sacarlal, J., Aponte, J.J., Leach, A., Macete, E., Aide, P., Sigauque, B., Milman, J., Mandomando, I., Bassat, Q., et al. (2005). Duration of protection with RTS,S/AS02A malaria vaccine in prevention of Plasmodium falciparum disease in Mozambican children: Single-blind extended follow-up of a randomised controlled trial. Lancet *366*, 2012–2018.

Bruna-Romero, O., Hafalla, J.C., Gonzalez-Aseguinolaza, G., Sano, G., Tsuji, M., and Zavala, F. (2001). Detection of malaria liver-stages in mice infected through the bite of a single Anopheles mosquito using a highly sensitive real-time PCR. Int. J. Parasitol. *31*, 1499–1502.

Cunha-Rodrigues, M., Prudencio, M., Mota, M.M., and Haas, W. (2006). Antimalarial drugs - host targets (re)visited. Biotechnol. J. *1*, 321–332.

Echeverri, C.J., Beachy, P.A., Baum, B., Boutros, M., Buchholz, F., Chanda, S.K., Downward, J., Ellenberg, J., Fraser, A.G., Hacohen, N., et al. (2006). Minimizing the risk of reporting false positives in large-scale RNAi screens. Nat. Methods *3*, 777–779.

Epiphanio, S., Mikolajczak, S.A., Goncalves, L.A., Pamplona, A., Portugal, S., Albuquerque, S., Goldberg, M., Rebelo, S., Anderson, D.G., Akinc, A., et al. (2008). Heme oxygenase-1 is an anti-inflammatory host factor that promotes murine plasmodium liver infection. Cell Host Microbe *3*, 331–338.

Franke-Fayard, B., Trueman, H., Ramesar, J., Mendoza, J., van der Keur, M., van der Linden, R., Sinden, R.E., Waters, A.P., and Janse, C.J. (2004). A Plasmodium berghei reference line that constitutively expresses GFP at a high level throughout the complete life cycle. Mol. Biochem. Parasitol. *137*, 23–33.

Goncalves, L.A., Vigario, A.M., and Penha-Goncalves, C. (2007). Improved isolation of murine hepatocytes for in vitro malaria liver stage studies. Malar. J. *6*, 169.

Greenwood, B., and Mutabingwa, T. (2002). Malaria in 2002. Nature *415*, 670–672.

Gu, X., Lawrence, R., and Krieger, M. (2000). Dissociation of the high density lipoprotein and low density lipoprotein binding activities of murine scavenger receptor class B type I (mSR-BI) using retrovirus library-based activity dissection. J. Biol. Chem. *275*, 9120–9130.

John, M., Constien, R., Akinc, A., Goldberg, M., Moon, Y.A., Spranger, M., Hadwiger, P., Soutschek, J., Vornlocher, H.P., Manoharan, M., et al. (2007). Effective RNAi-mediated gene silencing without interruption of the endogenous microRNA pathway. Nature *449*, 745–747.

Kocher, O., Yesilaltay, A., Cirovic, C., Pal, R., Rigotti, A., and Krieger, M. (2003). Targeted disruption of the PDZK1 gene in mice causes tissue-specific depletion of the high density lipoprotein receptor scavenger receptor class B type I and altered lipoprotein metabolism. J. Biol. Chem. *278*, 52820–52825.

Mazier, D., Beaudoin, R.L., Mellouk, S., Druilhe, P., Texier, B., Trosper, J., Miltgen, F., Landau, I., Paul, C., Brandicourt, O., et al. (1985). Complete development of hepatic stages of Plasmodium falciparum in vitro. Science *227*, 440–442.

Mota, M.M., Pradel, G., Vanderberg, J.P., Hafalla, J.C., Frevert, U., Nussenzweig, R.S., Nussenzweig, V., and Rodriguez, A. (2001). Migration of Plasmodium sporozoites through cells before infection. Science *291*, 141–144.

Nieland, T.J., Penman, M., Dori, L., Krieger, M., and Kirchhausen, T. (2002). Discovery of chemical inhibitors of the selective transfer of lipids mediated by the HDL receptor SR-BI. Proc. Natl. Acad. Sci. USA *99*, 15422–15427.

Nieland, T.J., Shaw, J.T., Jaipuri, F.A., Duffner, J.L., Koehler, A.N., Banakos, S., Zannis, V.I., Kirchhausen, T., and Krieger, M. (2008). Identification of the molecular target of small molecule inhibitors of HDL receptor SR-BI activity. Biochemistry *47*, 460–472.

Pamplona, A., Ferreira, A., Balla, J., Jeney, V., Balla, G., Epiphanio, S., Chora, A., Rodrigues, C.D., Gregoire, I.P., Cunha-Rodrigues, M., et al. (2007). Heme oxygenase-1 and carbon monoxide suppress the pathogenesis of experimental cerebral malaria. Nat. Med. *13*, 703–710.

Philips, J.A., Rubin, E.J., and Perrimon, N. (2005). Drosophila RNAi screen reveals CD36 family member required for mycobacterial infection. Science *309*, 1251–1253.

Prudencio, M., Rodriguez, A., and Mota, M.M. (2006). The silent path to thousands of merozoites: the Plasmodium liver stage. Nat. Rev. Microbiol. *4*, 849–856.

Prudencio, M., Rodrigues, C.D., Ataide, R., and Mota, M.M. (2008). Dissecting in vitro host cell infection by Plasmodium sporozoites using flow cytometry. Cell. Microbiol. *10*, 218–224.

Rhainds, D., Brodeur, M., Lapointe, J., Charpentier, D., Falstrault, L., and Brissette, L. (2003). The role of human and mouse hepatic scavenger receptor class B type I (SR-BI) in the selective uptake of low-density lipoprotein-cholesteryl esters. Biochemistry *42*, 7527–7538.

Scarselli, E., Ansuini, H., Cerino, R., Roccasecca, R.M., Acali, S., Filocamo, G., Traboni, C., Nicosia, A., Cortese, R., and Vitelli, A. (2002). The human scavenger receptor class B type I is a novel candidate receptor for the hepatitis C virus. EMBO J. *21*, 5017–5025.

Shakibaei, M., and Frevert, U. (1996). Dual interaction of the malaria circumsporozoite protein with the low density lipoprotein receptor-related protein (LRP) and heparan sulfate proteoglycans. J. Exp. Med. *184*, 1699–1711.

Silver, D.L. (2002). A carboxyl-terminal PDZ-interacting domain of scavenger receptor B, type I is essential for cell surface expression in liver. J. Biol. Chem. *277*, 34042–34047.

Silvie, O., Rubinstein, E., Franetich, J.F., Prenant, M., Belnoue, E., Renia, L., Hannoun, L., Eling, W., Levy, S., Boucheix, C., and Mazier, D. (2003). Hepatocyte CD81 is required for Plasmodium falciparum and Plasmodium yoelii sporozoite infectivity. Nat. Med. *9*, 93–96.

Silvie, O., Franetich, J.F., Boucheix, C., Rubinstein, E., and Mazier, D. (2007). Alternative invasion pathways for Plasmodium berghei sporozoites. Int. J. Parasitol. *37*, 173–182.

Sinnis, P., Willnow, T.E., Briones, M.R., Herz, J., and Nussenzweig, V. (1996). Remnant lipoproteins inhibit malaria sporozoite invasion of hepatocytes. J. Exp. Med. *184*, 945–954.

Van Eck, M., Hoekstra, M., Hildebrand, R.B., Yaong, Y., Stengel, D., Kruijt, J.K., Sattler, W., Tietge, U.J., Ninio, E., Van Berkel, T.J., and Pratico, D. (2007). Increased oxidative stress in scavenger receptor BI knockout mice with dysfunctional HDL. Arterioscler. Thromb. Vasc. Biol. *27*, 2413–2419.

Vishnyakova, T.G., Kurlander, R., Bocharov, A.V., Baranova, I.N., Chen, Z., Abu-Asab, M.S., Tsokos, M., Malide, D., Basso, F., Remaley, A., et al. (2006). CLA-1 and its splicing variant CLA-2 mediate bacterial adhesion and cytosolic bacterial invasion in mammalian cells. Proc. Natl. Acad. Sci. USA *103*, 16888–16893.